Material Design Strategy for Enhancement of Readback Signal Intensity in Ferroelectric Probe Data Storage

Yoshiomi Hiranaga and Yasuo Cho, *Member, IEEE*

***Abstract*— Ferroelectric probe data storage (FPDS) based on scanning nonlinear dielectric microscopy is expected as a next-generation data storage method with its large potential for improvement of the recording density. However, this novel method has a problem of low reading speed. To overcome this problem, a novel ferroelectric recording medium with large nonlinear permittivity is required because this data storage method uses the nonlinear dielectric response induced by small-amplitude ac bias to detect the bit data recorded in the form of polarization direction. Therefore, this article discusses nonlinear permittivity enhancement from the viewpoint of data storage application in the framework of the phenomenological theory. We reveal that the Curie-point control is one of the key techniques in material design for FPDS because nonlinear permittivity increases precipitously as the Curie temperature is approached, as with the linear permittivity and piezoelectric constants. A similar conclusion is also obtained through actual measurements of nonlinear permittivity in $LiTaO_3$ single crystals. On the other hand, we also reveal that there is a tradeoff relationship between nonlinear permittivity and polarization stability. To avoid this undesirable situation in data storage applications, pinning-site control will also be important. We also propose to employ a double-layer structure in the ferroelectric recording media for further improvement.**

***Index Terms*— Data storage systems, dielectrics, dielectric constant, ferroelectric devices, ferroelectric films, ferroelectric materials, frequency control, frequency modulation, RLC circuits, scanning probe data storage, temperature dependence.**

I. Introduction

FERROELECTRIC probe data storage (FPDS) based on scanning nonlinear dielectric microscopy (SNDM), in which ferroelectric material is used in the recording layer, has been proposed as a next-generation data storage method [1]–[4]. In this method, bit writing is conducted through the application of a local electric field to the recording layer using an ultrasharp conductive tip as a writing head and switching its polarization direction. To date, a demonstration has been reported that the data bit array with a recording density of 4 Tbit/in^2 has been successfully written using this method with a $LiTaO_3$ single crystal employed as a recording medium [3].

One of the most important technical subjects in the research and development for the practical realization of FPDS is to improve the readout speed. In ferroelectrics, the electric field created by spontaneous polarization is shielded by surface compensation charges, in contrast to ferromagnetics, in which no unipolar magnetic charge exists [5], [6]. This makes it difficult to detect the polarization direction directly. Thus, in FPDS, the polarization direction is detected in an indirect way using the nonlinear dielectric response while paying attention to the switching of the sign of nonlinear permittivity ε_{333} depending on the polarization direction in noncentrosymmetric materials. However, practically sufficient readback signal intensity has not yet been obtained, because ε_{333} of the existing recording media is extremely small [7].

Therefore, the development of novel ferroelectric recording media with large ε_{333} is the imminent issue in FPDS. However, ε_{333} has been paid little attention in typical ferroelectric and piezoelectric applications, and the material design strategy for tuning ε_{333} has not been established. Therefore, we focused on this point herein.

First, we formalized nonlinear permittivity based on the phenomenological theory. Although similar approaches are found in the earlier studies [8]–[10], we make a discussion from the viewpoint of the data storage application. We then conducted experimental measurements concerning the temperature dependence of ε_{333} in $LiTaO_3$ single crystals. We also discuss the influence of the Curie point (T_c) on ε_{333} through comparison between two different types of $LiTaO_3$ crystals. Finally, we discuss the material design strategy to realize high-speed reading in FPDS based on these theoretical and experimental results.

II. Phenomenological Theory of Nonlinear Permittivity

The origin of nonlinear permittivity is understood as the nonlinear response of polarization under an anharmonic potential. The potential curve of ferroelectrics has a double-minimum shape separated by an energy barrier ΔE, as shown in Fig. 1, which indicates ferroelectric bistability. This potential curve shows anharmonicity in the vicinity of the equilibrium point, and the degree of deviation from the harmonic potential corresponds to the nonlinear permittivity or nonlinear susceptibility $\chi^{(2)}$ ($\chi^{(2)} = \varepsilon_{333}/2\varepsilon_0$).

Manuscript received March 27, 2020; accepted June 30, 2020. Date of publication July 3, 2020; date of current version February 24, 2021. This work was supported in part by a Grant-in-Aid for Scientific Research from the Japan Society for the Promotion of Science (JSPS) under Grant 18K04932. *(Corresponding author: Yoshiomi Hiranaga.)*

The authors are with the Research Institute of Electrical Communication, Tohoku University, Sendai 980-8577, Japan (e-mail: hiranaga@riec.tohoku.ac.jp).

Digital Object Identifier 10.1109/TUFFC.2020.3006909

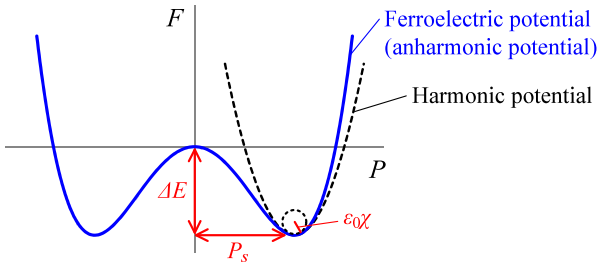

Fig. 1. Ferroelectric potential (anharmonic potential) curve and harmonic potential curve.

On the other hand, spontaneous polarization P_s is polarization at the local minimum point of the potential curve. The curvature of the potential curve at the equilibrium point accords to $\varepsilon_0\chi$, where χ is the linear susceptibility and ε_0 is the permittivity of a vacuum. ΔE is also an important parameter, which is associated with domain switching capability and domain stability.

The double-minimum potential shape allows us to presume that $\chi^{(2)}$ is not independent of P_s, χ, and ΔE, i.e., adequate control of P_s, χ, and ΔE is required to enhance $|\chi^{(2)}|$. (Note that the sign of $\chi^{(2)}$ for typical ferroelectrics is negative when $P_s > 0$.) Therefore, we derived the expression for the relationship among these parameters using a phenomenological approach.

First, we consider the second-order transition model. Using polarization P, the free energy F at temperature T is given by

$$F = \frac{\alpha_0(T - T_0)}{2}P^2 + \frac{\beta}{4}P^4 \tag{1}$$

where $\alpha_0 > 0$, $\beta > 0$, and T_0 is identical to T_c in the second-order transition model.

Using $\partial F/\partial P|_{P=P_s} = 0$ and $\partial P/\partial E|_{P=P_s} = \varepsilon_0\chi$, the following equations concerning P_s and χ are obtained:

$$P_s = \sqrt{\frac{\alpha_0}{\beta}}\sqrt{T_0 - T} \tag{2}$$

$$\chi = \frac{1}{2\varepsilon_0\alpha_0(T_0 - T)}. \tag{3}$$

Substituting (2) into (1) by letting $P = P_s$, ΔE is then written as

$$\Delta E = \frac{\alpha_0^2(T_0 - T)^2}{4\beta}. \tag{4}$$

On the other hand, by repeating derivation with respect to P and E, we obtain

$$\alpha_0(T_0 - T)\frac{\partial^2 P}{\partial E^2} + 6\beta P\left(\frac{\partial P}{\partial E}\right)^2 + 3\beta P^2\frac{\partial^2 P}{\partial E^2} = 0. \tag{5}$$

Considering $\partial^2 P/\partial E^2|_{P=P_s} = 2\varepsilon_0\chi^{(2)}$, $\chi^{(2)}$ is given from this equation as

$$\chi^{(2)} = -3\varepsilon_0^2\beta P_s\chi^3 \tag{6}$$

where we also used (2) and (3) to rearrange the equation. This equation is known as Miller's formula [11]. Using (3) and (4), this equation is rewritten as

$$\chi^{(2)} = -\frac{3}{16}\frac{P_s\chi}{\Delta E}. \tag{7}$$

Hence, $\chi^{(2)}$ is proportional to P_s and χ, and is inversely proportional to ΔE. This corresponds to our instinctive understanding from Fig. 1.

Moreover, substituting (2)–(4), (7) is also rewritten as

$$\chi^{(2)} = -\frac{3\beta^{1/2}}{8\varepsilon_0\alpha^{5/2}}\frac{1}{(T_0 - T)^{5/2}}. \tag{8}$$

Hence, $\chi^{(2)}$ is inversely proportional to $(T_0 - T)^{5/2}$. Therefore, the control of T_c is effective to enhance $|\chi^{(2)}|$. (Remember that $T_0 = T_c$ in the second-order transition model.) T_c control through dopant addition is a very common method to enhance the linear permittivity and piezoelectric constants [12]. A similar strategy is considered to be available for $|\chi^{(2)}|$ enhancement.

On the other hand, we must pay attention to some tradeoff relationship when $|\chi^{(2)}|$ is increased in accordance with such a concept. According to (7), an increase in P_s is effective to enhance $|\chi^{(2)}|$. However, even in $PbTiO_3$, which has the largest P_s in typical ferroelectrics known to date, P_s is approximately 100 μC/cm^2 [13], and it seems to be difficult to obtain a novel ferroelectric material that has a much larger P_s than this. This value is no more than twice as large as P_s of the current recording media [e.g., $LiTaO_3$ and lead zirconate titanate (PZT)]. Therefore, a drastic improvement will not be expected through control of P_s. On the other hand, decreasing ΔE is an alternative way to enhance $|\chi^{(2)}|$. However, this approach will also naturally confront the other limitation because an excessive decrease of ΔE will cause a severe problem with regard to data retention. The control of χ while maintaining P_s and ΔE, thus, seems to be the only way to enhance $|\chi^{(2)}|$ without degradation of data retention. However, this approach will also confront a similar limitation. In the second-order transition model, χ, P_s, and ΔE are not independent of each other. These variables are connected by the relation

$$\chi = \frac{P_s^2}{8\varepsilon_0\Delta E}. \tag{9}$$

Using this relation, (7) is rewritten again as

$$\chi^{(2)} = -\frac{3P_s^3}{128\varepsilon_0\Delta E^2}. \tag{10}$$

This equation indicates that it is difficult, in principle, to enhance $|\chi^{(2)}|$ unless ΔE is decreased, i.e., it suggests that there is a tradeoff relationship between improving the readout speed and ensuring data retention in FPDS. The specific tactics to avoid this problem will be discussed in Section IV.

While this discussion has assumed the second-order transition model, we also reach similar conclusions with the first-order transition model, except for the change in the expression of $\chi^{(2)}$. The free energy for the first-order transition model is given as

$$F = \frac{\alpha}{2}P^2 + \frac{\beta}{4}P^4 + \frac{\gamma}{6}P^6 \tag{11}$$

where $\alpha = \alpha_0(T - T_0)$, $\alpha_0 > 0$, $\beta < 0$, and $\gamma > 0$. Unlike the second-order transition model, T_0 does not accord to T_c for the first-order transition model. In a similar manner, we have

the following expressions that concern P_s, χ, ΔE, and $\chi^{(2)}$ in a ferroelectric phase:

$$P_s = \sqrt{\frac{-\beta + \sqrt{\beta^2 - 4\alpha\gamma}}{2\gamma}} \tag{12}$$

$$\chi = \frac{1}{-4\varepsilon_0\alpha - 2\beta\varepsilon_0 P_s^2} \tag{13}$$

$$\Delta E = \frac{\beta - \sqrt{\beta^2 - 4\alpha\gamma}}{4\gamma}\left(\frac{2\alpha}{3} + \frac{-\beta^2 - \beta\sqrt{\beta^2 - 4\alpha\gamma}}{12\gamma}\right) \tag{14}$$

$$\chi^{(2)} = -\frac{9\varepsilon_0\chi^2}{2P_s} + \frac{24\varepsilon_0^2\chi^3\Delta E}{P_s^3}. \tag{15}$$

Equation (15) has a complicated form, unlike (7). This formula may give a peculiar impression because this formula allows $\chi^{(2)}$ to be positive when the absolute value of the second term is larger than that of the first term, while the experimentally obtained $\chi^{(2)}$ is always negative [14], [15]. If $\chi^{(2)}$ is permitted to be positive, $|\chi^{(2)}|$ must increase with ΔE. However, this cannot happen in reality. In this way, (15) appears to include a contradiction at first glance; however, the right-hand side of (15) does not take a positive value when considering the allowed range of each variable, and thus, $|\chi^{(2)}|$ decreases monotonically with an increase in ΔE. Indeed, in the first-order transition model, χ, P_s, and ΔE are independent variables, unlike the second-order transition model, but the allowable ranges of χ and ΔE are limited as

$$0 < \chi < \frac{P_s^2}{8\varepsilon_0\Delta E} \tag{16}$$

$$0 \le \Delta E < \frac{P_s^2}{8\varepsilon_0\chi}. \tag{17}$$

Due to these regulations, the right-hand side of (15) is confined to be negative. The range of the absolute value of $|\chi^{(2)}|$ is also limited as

$$|\chi^{(2)}| < \frac{3P_s^3}{128\varepsilon_0\Delta E^2}. \tag{18}$$

Therefore, the maximum value of $|\chi^{(2)}|$ for the first-order transition model accords to (10), which is for the second-order transition model, i.e., the tradeoff relationship between readout speed and data retention also lies on the first-order transition model.

III. Actual Measurements of Nonlinear Permittivity

The temperature dependence of the nonlinear permittivity of $LiTaO_3$ single crystals was experimentally investigated. $LiTaO_3$ is one of the most important materials for ferroelectric recording media for FPDS because it is the first material that achieved a recording density greater than 1 Tbit/in^2. This material is also advantageous to study intrinsic nonlinear permittivity because high-quality single crystals are available. In contrast, in measurements of thin films or ceramics, the measured signal often contains extrinsic nonlinear permittivity derived from grains and domain boundaries in addition to intrinsic nonlinear permittivity [7], [16]. The readout speed

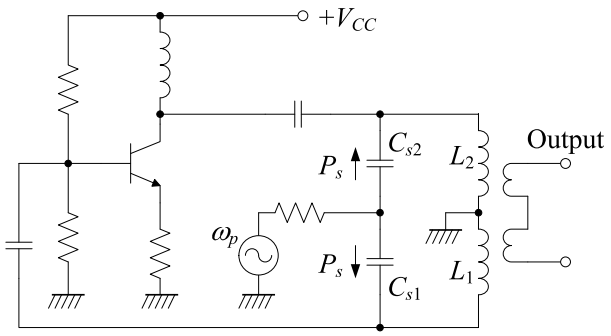

Fig. 2. Testing circuit used for the dynamic measurement method.

is associated with intrinsic nonlinear permittivity because it determines the polarity of each written bit. It is not impossible, in principle, but difficult to separate the intrinsic component from the extrinsic component in measurements of thin films and ceramics. In contrast, measured signals with polarized single crystals can be regarded to originate from only intrinsic nonlinear permittivity.

In this study, two types of crystals having slightly different composition ratios were used. The first crystal is stoichiometric $LiTaO_3$ (SLT), [Li] : [Ta] of which is strictly 1 : 1 [17]. The second crystal is congruent $LiTaO_3$ (CLT) with [Li] : [Ta] = 48.6 : 51.4. CLT crystals have many Li point defects due to the disproportion between Li and Ta. The Li defects act as pinning sites and have a significant influence on the domain switching properties. There is a large difference in the coercive field E_c between SLT and CLT ($E_c < 20$ kV/cm for SLT, and $E_c \sim 100$ kV/cm for CLT [17]). The difference in the [Li] : [Ta] ratio also has a considerable effect on T_c. CLT has an 80 °C lower T_c than SLT, in which T_c is 685 °C.

Nonlinear permittivity measurements were conducted using the dynamic measurement method with the measurement circuit illustrated in Fig. 2 [18]. The measurement circuit is based on a Hartley oscillator with an LC resonator. The LC resonator consists of two capacitors, C_{s1} and C_{s2}, which are made of the ferroelectric materials to be measured, and two embedded inductances, L_1 and L_2. The resonant frequency is given by

$$f_0 = \frac{1}{2\pi\sqrt{L(C_s + C_{\rm st})}} \tag{19}$$

where $L = L_1 + L_2$, $C_s = C_{s1}C_{s2}/(C_{s1} + C_{s2})$, and $C_{\rm st}$ is the stray capacitance. The midpoint of C_{s1} and C_{s2} is connected to an ac voltage source. When a small ac voltage is applied to the measurement samples, the capacitance changes slightly due to the nonlinearity of the samples, and the oscillating frequency f_0 changes periodically, i.e., the output signal of the oscillating circuit generates an FM signal. ε_{333} of the sample can be evaluated quantitatively by analysis of this FM spectrum.

Fig. 3(a) shows an example of measured FM spectra for CLT at room temperature. The spectrum intensity ratio of the carrier and the sideband wave gives the modulation index m_f, which is converted into ε_{333} as

$$|\varepsilon_{333}| = \frac{C_s + C_{\rm st}}{C_s}\frac{2\varepsilon_{33}f_p m_f}{f_0 E_p} \tag{20}$$

where f_p and E_p are the frequency and the intensity of the ac bias field, respectively, and ε_{33} [$= \varepsilon_0(1 + \chi)$] is the

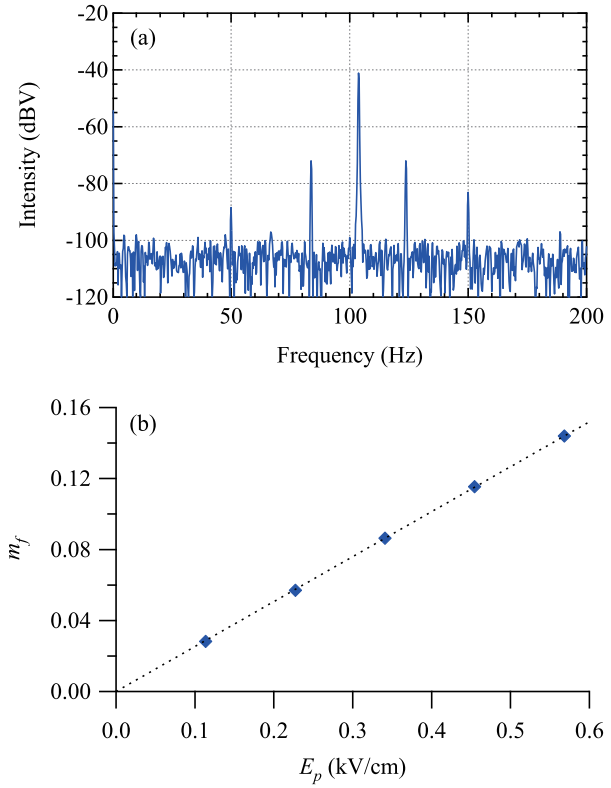

Fig. 3. (a) FM spectrum by the dynamic measurement method observed for a $LiTaO_3$ single crystal. (b) Modulation index m_f calculated from the obtained FM spectrum as a function of the applied electric field, E_p.

linear permittivity. $(C_s + C_{st})/C_s$ is a calibration factor related to the stray capacitance [7]. The linear relationship between m_f and E_p was confirmed for this experiment, as shown in Fig. 3(b), which suggests that the contribution of an extrinsic nonlinear response is negligible in this measurement. The calculated value of ε_{333} for CLT by this measurement was -0.73 aF/V. (The sign of ε_{333} was determined from the phase difference between the applied bias field and the demodulated signal.)

This measurement value can be compared with a value predicted in a different way. Elimination of ΔE from (7) and (9) gives the following relationship:

$$\chi^{(2)} = -\frac{3\varepsilon_0 \chi^2}{2P_s}. \tag{21}$$

By substituting literature values, $\chi = 42.4$ and $P_s = 60\ \mu C/cm^2$ [17], ε_{333} is estimated to be -0.70 aF/V for CLT, which is in good agreement with the measurement value, although the phenomenological formalization contains a rough approximation.

The measured temperature dependence of ε_{333} for SLT and CLT is shown in Fig. 4(a). This graph clarified that $|\varepsilon_{333}|$ increases divergently with temperature for both crystals, as predicted by (8). The difference in the properties between SLT and CLT is explained by the difference in their T_c values, i.e., $|\varepsilon_{333}|$ of CLT increases at a lower temperature because of its lower T_c compared with SLT. In other words, CLT has a larger $|\varepsilon_{333}|$ than SLT at a fixed temperature.

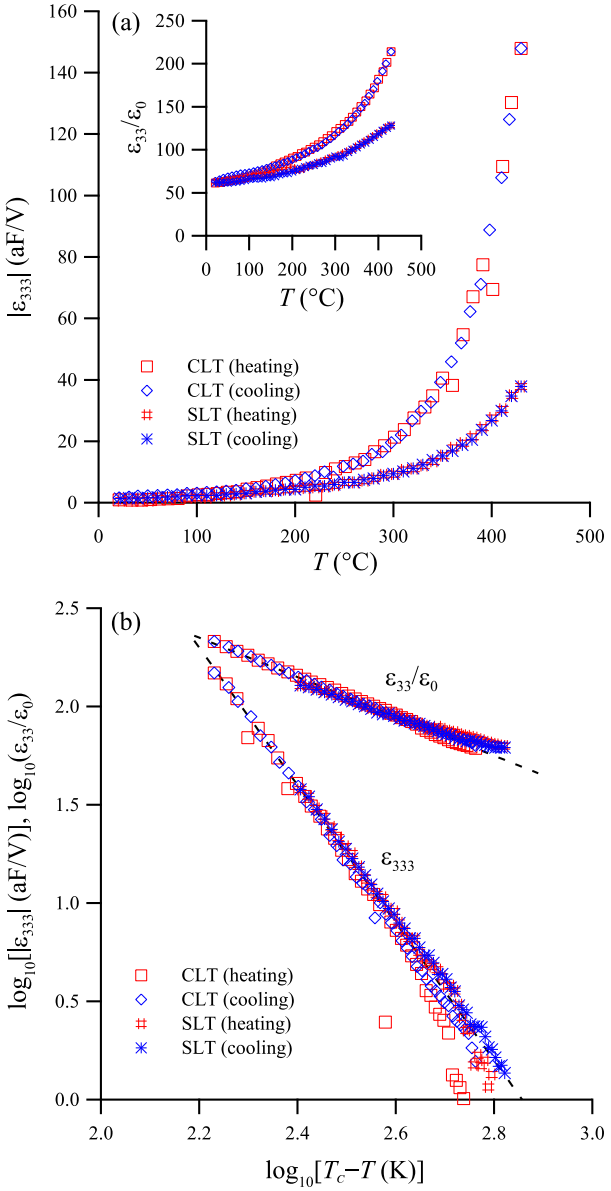

Fig. 4. (a) Nonlinear permittivity ε_{333} and linear permittivity ε_{33} (inset graph) for SLT and CLT single crystals as a function of temperature T. (b) Logarithmic chart.

The logarithmic chart of the temperature dependence is shown in Fig. 4(b). Both the linear and nonlinear permittivities are plotted linearly on the double-logarithmic chart. However, the slopes are different: The nonlinear permittivity has a larger slope and greater dependence on the temperature. ε_{333} for SLT and CLT is aligned on an identical line in this chart. Note that the horizontal axis does not represent $\log T$, but $\log(T_c - T)$. Therefore, the difference in ε_{333} between the two crystals is thoroughly attributable to the T_c shift.

ε_{333} is plotted linearly on the double-logarithmic chart so that it is expressed as $\varepsilon_{333} \propto (T_c - T)^{-\mu}$. However, the experimentally obtained μ was 3.5, which disagrees with the theoretical value of 2.5. The cause of this disagreement has yet to be determined. Nevertheless, this experimental demonstration of the explosive increase of $|\varepsilon_{333}|$ with temperature gives important insight for FPDS.

IV. Material Design Strategy for Ferroelectric Recording Media

Following the theoretical and experimental results, we discuss the material design strategy for recording media of FPDS in this section.

Both the theoretical and experimental results indicated that the nonlinear permittivity has a large dependence on the temperature. Therefore, the control of T_c through composition tuning can be an effective means to enhance the nonlinear permittivity, as found in the comparison between SLT and CLT. Similar control is realized through dopant addition. In fact, we confirmed that Sr-doped PZT has a larger ε_{333} than nondoped PZT; the details of this latest study will be discussed elsewhere.

On the other hand, there is a concern that lowering T_c impairs domain stability, which is unfavorable for data storage applications. This is the dilemma itself found in (10) and (18).

One of the keys to overcoming this dilemma is a pinning-site control approach. Remember that CLT exhibits a far larger E_c than SLT without the cost of ε_{333}. There is no significant difference between SLT and CLT, or rather, CLT has a slightly larger ε_{333} at room temperature, whereas for E_c, there is more than a tenfold difference between SLT and CLT. In other words, the accurate introduction of pinning sites is proved to enable the domain stability to be improved independently of the nonlinear permittivity. The difference in the temperature dependence of ε_{333} between SLT and CLT does not exceed the difference derived from the difference in T_c, which suggests that intrinsic nonlinear permittivity and the pinning-site effect are essentially unrelated.

Further effects are expected when these two approaches are integrated into double-layer media. The readback signal of FPDS is determined by the physical properties of the uppermost surface of the recording media because the electric field is highly concentrated in the vicinity of the probe apex [19]. In contrast, the domain stability is contributed by the entire recording layer in the thickness direction because the switched domain must penetrate through the ferroelectric layer to be stabilized [20]. Considering this, we devised an ideal structure for ferroelectric recording media. The double-layer recording media contains a “soft" ferroelectric film with a large ε_{333} as the top layer and a “hard” ferroelectric film with a large E_c as the bottom layer. This combination will make the most of the benefits of both materials at the same time. The top layer will enhance the readback signal intensity. The low E_c of the top layer will not become fatal to data retention because its domain instability will be compensated by the bottom layer. The proposed concept is summarized in Fig. 5.

This concept will broaden the range of material selection because it will allow each layer to be selected independently. Although, as repeatedly mentioned, $LiTaO_3$ is advantageous from the viewpoint of recording density, it has not been regarded as the favorite recording media in single-layer recording media because of its low ε_{333}. However, in the framework of the double-layer concept, $LiTaO_3$ becomes a promising candidate for the hard material of the bottom layer. HfO_2-based ferroelectrics, which have attracted increased attention lately, also do not have sufficient ε_{333}, while this

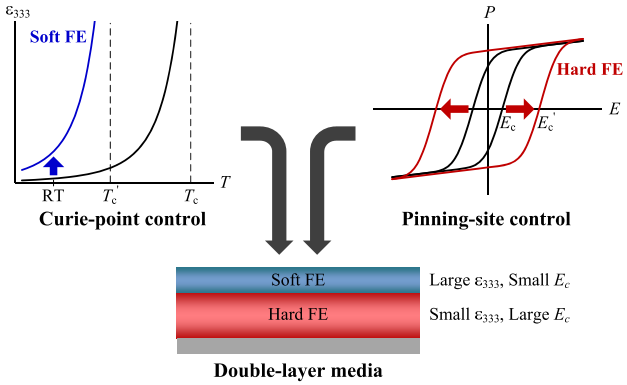

Fig. 5. Overview of the material design strategy for recording media of FPDS.

family of ferroelectrics has favorable characteristics in that the ferroelectricity does not disappear in the very low (< 10 nm) film-thickness range [21], [22]. The double-layer concept will also lower the threshold for the adoption of such novel-type ferroelectrics.

The design freedom of the soft layer will also be increased by the double-layer structure. ε_{333} is inversely proportional to $(T_0 - T)^{\mu}$; therefore, ferroelectrics with T_c close to room temperature have larger ε_{333} by orders of magnitude. However, domains in such ferroelectrics could be quite unstable. If such an unstable domain can be stabilized by the underlying hard layer, then T_c of the top layer will be allowed to be lowered to the vicinity of room temperature. This has the potential to provide clues as how to significantly improve the readout speed of FPDS.

When T_c is set near the room temperature, the readback signal from the soft ferroelectrics has a large temperature dependence. This is undesirable in practical use. To compensate for this drawback, it may be necessary to implement some kind of temperature compensation circuit. Nevertheless, since bit readout operation is in principle achieved by sign discrimination with 0 V as the threshold, the level fluctuations in the readback signal are tolerable to some extent.

On the fabrication of the ferroelectric double layer, the soft and hard layers should have P_s with the same magnitude. Otherwise, the interface has a charge mismatch, which has a significant effect on the polarization switching. On the other hand, the control of T_c without the change of P_s is not easy. This, however, does not mean the difficulty in the realization of the double-layer recording media because it is possible to choose a combination of soft and hard materials having P_s with the same magnitude from a wide variety of ferroelectrics. For instance, PZT and $LiTaO_3$ have ε_{333} and E_c with quite different magnitudes, whereas there is no significant difference between these materials in terms of P_s [7], [17], [23]. Similarly, $BaTiO_3$ single crystals and yttrium-doped HfO_2 thin films have the almost same P_s, whereas E_c of these materials differ by three to four orders of magnitude [24], [25].

V. Conclusion

A methodology for enhancement of the intrinsic nonlinear permittivity with an aim to improve readout speed in FPDS was explored. In both the theory based on

the phenomenological approach and experiments using single-crystal $LiTaO_3$, nonlinear permittivity is revealed to be inversely proportional to $(T_0-T)^{\mu}$ although the specific values of μ are different between the two. Therefore, the Curie-point control is effective to enhance nonlinear permittivity. On the other hand, there is a tradeoff relationship between the nonlinear permittivity and potential barrier, and it seems to be difficult to improve readout speed without degradation of the bit retention property. The keys to overcoming this dilemma will be pinning-site control and double-layer recording media. We are expectant that the prominent combinations of base and dopant materials will be found for both soft and hard layers in double-layer recording media, which will cause a breakthrough in this field.

REFERENCES

[1] Y. Hiranaga, Y. Cho, K. Fujimoto, Y. Wagatsuma, and A. Onoe, "Ultrahigh-density ferroelectric data storage using scanning nonlinear dielectric microscopy," *Jpn. J. Appl. Phys.*, vol. 42, no. 1, pp. 6050–6054, Sep. 2003.

[2] Y. Hiranaga, T. Uda, Y. Kurihashi, H. Tochishita, M. Kadota, and Y. Cho, "Nanodomain formation on ferroelectrics and development of hard-disk-drive-type ferroelectric data storage devices," *Jpn. J. Appl. Phys.*, vol. 48, no. 1, 2009, Art. no. 09KA18.

[3] K. Tanaka and Y. Cho, "Actual information storage with a recording density of 4 Tbit/in.^{2} in a ferroelectric recording medium," *Appl. Phys. Lett.*, vol. 97, no. 9, pp. 92901–92903, 2010.

[4] T. Aoki, Y. Hiranaga, and Y. Cho, "High-density ferroelectric recording using a hard disk drive-type data storage system," *J. Appl. Phys.*, vol. 119, no. 18, May 2016, Art. no. 184101.

[5] S. V. Kalinin and D. A. Bonnell, "Local potential and polarization screening on ferroelectric surfaces," *Phys. Rev. B, Condens. Matter*, vol. 63, no. 12, Mar. 2001, Art. no. 125411.

[6] M. G. Forrester *et al.*, "Charge-based scanning probe readback of nanometer-scale ferroelectric domain patterns at megahertz rates," *Nanotechnology*, vol. 20, no. 22, Jun. 2009, Art. no. 225501.

[7] Y. Hiranaga and Y. Cho, "Measurements of nonlinear dielectric constants of $Pb(Zr,Ti)O_3$ thin films using a dynamic measuring method," *Jpn. J. Appl. Phys.*, vol. 52, no. 9, 2013, Art. no. 09KA08.

[8] S. Ikeda, H. Kominami, K. Koyama, and Y. Wada, "Nonlinear dielectric constant and ferroelectric–to–paraelectric phase transition in copolymers of vinylidene fluoride and trifluoroethylene," *J. Appl. Phys.*, vol. 62, no. 8, pp. 3339–3342, Oct. 1987.

[9] M. Iwata, R. Kamei, H. Orihara, Y. Ishibashi, H. Ohwa, and N. Yasuda, "Nonlinear dielectric response in relaxor ferroelectrics $(1-x)Pb(Mg_{1/2}W_{1/2})O_3$-$xPbTiO_3$ $(x = 0.5)$," *Jpn. J. Appl. Phys.*, vol. 37, no. 1, pp. 5413–5417, 1998.

[10] A. E. Glazounov and A. K. Tagantsev, "Phenomenological model of dynamic nonlinear response of relaxor ferroelectrics," *Phys. Rev. Lett.*, vol. 85, no. 10, pp. 2192–2195, Sep. 2000.

[11] R. C. Miller, "Optical second harmonic generation in piezoelectric crystals," *Appl. Phys. Lett.*, vol. 5, no. 1, pp. 17–19, Jul. 1964.

[12] Y. Xu, *Ferroelectric Materials and Their Applications*. Amsterdam, The Netherlands, North Holland, 1991.

[13] T. Morita and Y. Cho, "Epitaxial $PbTiO_3$ thin films on $SrTiO_3(100)$ and $SrRuO_3/SrTiO_3(100)$ substrates deposited by a hydrothermal method," *Jpn. J. Appl. Phys.*, vol. 43, no. 9, pp. 6535–6538, 2004.

[14] Y. Cho, "Determination of electrostrictive and third-order dielectric constants of piezoelectric ceramic," *Jpn. J. Appl. Phys.*, vol. 39, no. 1, pp. 3524–3527, Jun. 2000.

[15] S. Kazuta, Y. Cho, and H. Odagawa, "Determination of crystal polarities of piezoelectric thin film using scanning nonlinear dielectric microscopy," *J. Eur. Ceram. Soc.*, vol. 21, nos. 10–11, pp. 1581–1584, Jan. 2001.

[16] D.-J. Kim, J.-P. Maria, A. I. Kingon, and S. K. Streiffer, "Evaluation of intrinsic and extrinsic contributions to the piezoelectric properties of $Pb(Zr_{1-x}T_x)O_3$ thin films as a function of composition," *J. Appl. Phys.*, vol. 93, no. 9, pp. 5568–5575, May 2003.

[17] K. Kitamura, Y. Furukawa, K. Niwa, V. Gopalan, and T. E. Mitchell, "Crystal growth and low coercive field 180° domain switching characteristics of stoichiometric $LiTaO_3$," *Appl. Phys. Lett.*, vol. 73, no. 21, pp. 3073–3075, Nov. 1998.

[18] Y. Cho and F. Matsuno, "Dynamic measuring method of capacitance variation of piezoelectric ceramics with alternating electric field," *Jpn. J. Appl. Phys.*, vol. 31, no. 1, pp. 3627–3631, Nov. 1992.

[19] K. Ohara and Y. Cho, "Fundamental study of surface layer on ferroelectrics by scanning nonlinear dielectric microscopy," *Jpn. J. Appl. Phys.*, vol. 40, no. 1, pp. 5833–5836, Sep. 2001.

[20] Y. Daimon and Y. Cho, "Cross-sectional observation of nanodomain dots formed in both congruent and stoichiometric $LiTaO_3$ crystals," *Appl. Phys. Lett.*, vol. 90, no. 19, pp. 192903–192906, 2007.

[21] M. H. Park, Y. H. Lee, H. J. Kim, Y. J. Kim, T. Moon, K. D. Kim, J. Müller, A. Kersch, U. Schroeder, T. Mikolajick, and C. S. Hwang, "Ferroelectricity and antiferroelectricity of doped thin HfO_2-based films," *Adv. Mater.*, vol. 27, no. 11, pp. 1811–1831, Mar. 2015.

[22] Y. Hiranaga, T. Mimura, T. Shimizu, H. Funakubo, and Y. Cho, "Dynamic observation of ferroelectric domain switching using scanning nonlinear dielectric microscopy," *Jpn. J. Appl. Phys.*, vol. 56, no. 10S, 2017, Art. no. 10PF16.

[23] C. M. Foster *et al.*, "Single-crystal $Pb(Zr_xTi_{1-x})O_3$ thin films prepared by metal-organic chemical vapor deposition: Systematic compositional variation of electronic and optical properties," *J. Appl. Phys.*, vol. 81, no. 5, pp. 2349–2357, Mar. 1997.

[24] W. J. Merz, "Double hysteresis loop of $BaTiO_3$ at the Curie point," *Phys. Rev.*, vol. 91, no. 3, pp. 513–517, Aug. 1953.

[25] J. Müller *et al.*, "Ferroelectricity in yttrium-doped hafnium oxide," *J. Appl. Phys.*, vol. 110, no. 11, 2011, Art. no. 114113.

Yoshiomi Hiranaga was born in Japan in 1979. He received the Ph.D. degree in electronic engineering from Tohoku University, Sendai, Japan, in 2006.

He is currently an Assistant Professor with the Research Institute of Electrical Communication, Tohoku University. His research interests include domain switching phenomena on ferroelectric materials in the nanoscale area and their applications for next-generation high-density data storage devices.

Yasuo Cho (Member, IEEE) graduated from the Electrical Engineering Department, Tohoku University, Sendai, Japan, in 1980.

In 1985, he became a Research Associate with the Research Institute of Electrical Communication, Tohoku University. In 1990, he received an Associate Professorship from Yamaguchi University, Yamaguchi, Japan. He then became an Associate Professor in 1997 and a Full Professor in 2001 at the Research Institute of Electrical Communication, Tohoku University, where he is currently a Professor. During this time, his main research interests include nonlinear phenomena in ferroelectric materials and their applications, research on the scanning nonlinear dielectric microscopy (SNDM), development on novel evaluation methods of semiconductor materials and devices based on SNDM, and research on using the SNDM in next-generation ultrahigh density ferroelectric data storage (SNDM ferroelectric probe memory).